Chapter 3

Isolation of cellulose from lignocellulosic feedstocks (Saccharum spontaneum and Banana agrowastes) using an integrated pretreatment technique: Process optimization and structural characterization

Abstract

An integrated treatment coupling alkali, steam explosion, and ammonia/chlorine-free bleaching with sequential mild acid pretreatment were performed to isolate and characterize cellulose from *Saccharum spontaneum* (*S. spontaneum*) and banana agrowastes. The cellulose yield, compositional, microstructural, and morphological analysis initially obtained from *S. spontaneum* and three post-harvest banana agrowastes (peel, pseudostem, and peduncle) were surveyed. Isolation parameters for *S. spontaneum* and banana peduncle agrowaste, the most efficient precursors, were reconfigured for acid hydrolysis by applying an orthogonal L_9 array of Taguchi design to attain high-quality cellulose with the highest yield. The cellulose source at its different stages of processing was submitted to various analytical techniques for morphological and physiochemical investigations. Effects of solution-to-pulp ratio, acid concentration, temperature, and reaction time on physicochemical parameters were assessed resulting in ~83% cellulose recovery from *S. spontaneum* and ~81% from banana peduncle. Detailed analyses showed that the isolated cellulose has good crystallinity and thermal stability with lower DP levels that offer more binding sites for enzymes, boosting the rate of downstream hydrolysis.

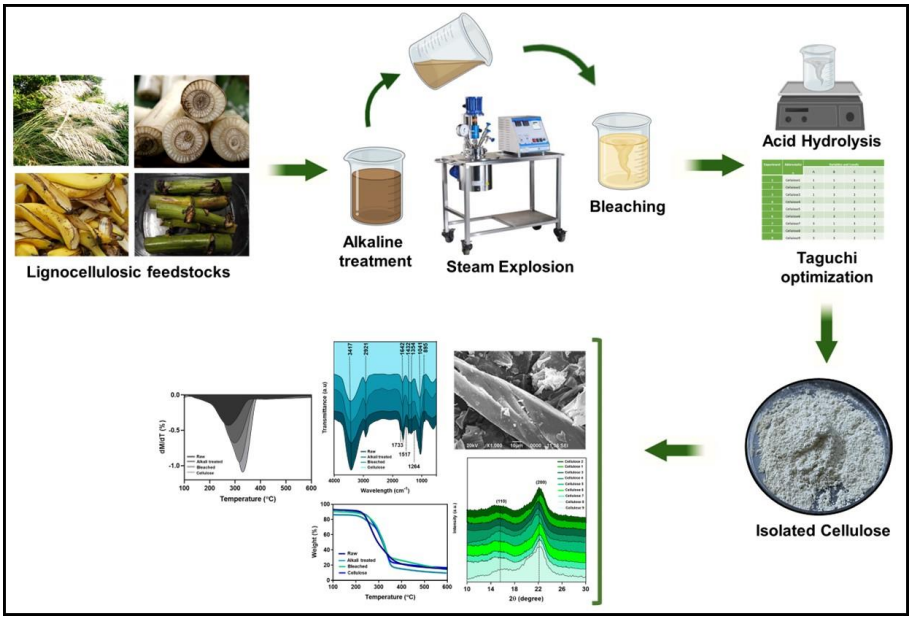

3.1. Introduction

Growing global environmental concerns, as well as emerging environmental restrictions, have driven the quest for environmentally friendly materials. Cellulose, the most abundant biopolymer, has piqued the interest of researchers due to its biodegradability, biocompatibility, sustainability, and renewability, and is currently being recognized as a green alternative to fossil fuels-based polymers [1]. Chemically, cellulose is a linear homopolymer of glucose $(C_6H_{10}O_5)_n$ with monomer units of *d*-glucose in a $^4C_1$ configuration that is water insoluble but hydrolyzed by microbial and fungal enzymes [2]. Cellulose can be sourced from diverse natural precursors, among which, plant biomass is the most abundant and readily available, and so has the most potential for substantial production of cellulose. For instance, cellulose has been successfully isolated from sugarcane bagasse [3], rice straw [4], kenaf [5], rice husk [6], and wood [7]. Since these lignocellulosic agricultural residues are mainly composed of cellulose, hemicellulose, and lignin, therefore efficient separation is the primary challenge before converting them to useful chemicals [8].

Saccharum spontaneum (S. spontaneum), also known as Kans grass is a perennial herbaceous plant belonging to the *Poaceae* family that grows rapidly on non-agricultural lands alongside roads, canals, and river banks. The grass does not hold much commercial value presently and is widely distributed in Asia, the Mediterranean regions, and the warm temperate regions of Africa [9]. *S. spontaneum* has been reported to contain 45.10 ± 0.35 % of cellulose and 22.75 ± 0.28 % hemicellulose on a dry solid basis [10]. Due to its high cellulosic and hemicellulosic content it has become popular as a renewable bioresource for the production of second-generation ethanol [11, 12, 13] and the preparation of green polymer composites [14, 15, 16]. Although, one recent report has demonstrated the potential industrial application of *S. spontaneum*, where it was used for the isolation of chlorine-free bleached pulp for the paper industry, the isolation of cellulosic fibers remains unexplored [17]. Similarly, banana agrowastes despite being one of the most abundant lignocellulosic sources remain underutilized [18]. Bananas are widely cultivated in Asia, Latin America, and Africa with an annual production of over 116 million metric tonnes (MMT) globally and account for 16% of the total global food production. India is currently the highest producer with 27.9 MMT, followed by China, (10.1 MMT), and the Philippines (7.8 MMT) [19]. Consequently, the agrowastes generated thereof (banana peduncle, peels,

leaves, and pseudostems) accumulate in enormous quantities, whereas it could serve as a viable lignocellulosic feedstock [20].

Given that celluloses in lignocellulosic agrowaste are imperviously interwoven within matrices of hemicelluloses and lignin, isolation mandates pre-treatments for reorganizing the inter-and intramolecular hydrogen bond network, the shape of cellulose, as well as lignin removal [21]. Some pre-treatment strategies including acid pre-treatment, alkali pre-treatment, and organic solvent pre-treatment, have been developed in several studies to fractionate hemicellulose and lignin for the extraction of cellulose [22, 23]. Acid hydrolysis, particularly with H_2SO_4 and HCl, is considered safer owing to its fewer negative environmental impacts. Haafiz et al. (2013) reported oil palm empty fruit bunch hydrolysis using 2.5 N HCl [24], while Maiti et al. (2013) reported waste paper hydrolysis using 47% H_2SO_4 [25]. Meanwhile, Morais et al., (2013) reported the extraction of cellulose from raw cotton linter using 64% H_2SO_4. Despite its potential, an acid concentration above 60% is not recommended due to the inhibition of downstream enzymatic processes, environmental damage, and the corrosion caused to the extraction equipment [26]. The ammonia/chlorine-based oxidation agent in such pre-treatments effectively bleaches cellulose fibers and improves cellulose fibrillation. Nevertheless, there is always the possibility of ammonia/chlorine leakage, related toxicity, groundwater contamination, malodorousness, and carcinogenesis [27]. Additionally, the vastly organized crystalline structure of celluloses derived through conventional acid-alkali pre-treatments having a high degree of polymerization and low surface-to-volume ratios precludes the interaction of their β-(1,4)-glycosidic linkages with enzymes, making it resistant to enzymatic hydrolysis [28]. Therefore, the current isolation trends are refocusing on the use of sustainable and environment-friendly processes.

In this chapter, we have reported a simple and sustainable process of cellulose isolation from *S. spontaneum* and banana agrowastes by introducing successive treatments of alkali, steam explosion, and total-chlorine-free bleaching along with the acid hydrolysis step. It is important to emphasize that the production of cellulose from *S. spontaneum* and banana agrowastes using this multiple-step method requires a significantly lower quantity of reagents and generates very low effluents from material washes that make the process more economical and environment-friendly. The four parameters (acid concentration reaction time, temperature, and pulp-solution ratio) that could possibly influence the efficiency of extraction during acid hydrolysis were assessed and the Taguchi orthogonal

array used for the statistical design of experiment was conducted to optimize the hydrolysis conditions. The structure, crystallinity, and thermal stability of the raw and extracted cellulose were analyzed for the comparative assessment of the primary characteristics at different stages of isolation to correlate it with the optimized process for isolation.

3.2. Materials and methods

3.2.1. Materials and chemicals

S. spontaneum (Kans grass) was collected from Napaam area, Tezpur, Assam, India in the month of September, 2017 after full maturity. Agrowastes (peel, pseudostem, and peduncle) from the widely available banana cultivar (*Musa* spp.), Dwarf Cavendish (local name: "Jahaji"), were collected from local plantations of the Napaam area of Tezpur, Assam, India in 2017. Sodium hydroxide (NaOH), Hydrogen peroxide (H_2O_2), and Sulphuric acid (H_2SO_4) were purchased from Merck Pvt. Ltd., India.

3.2.2. Preparation of raw material

The *S. spontaneum* and banana agrowastes were chopped separately into small pieces (1-2 cm) and washed thoroughly with distilled water for the removal of any surface impurities. After cutting and washing, the samples were kept in a hot air oven at a temperature of 80°C to attain uniform moisture content. The dried samples were then ground to powder using a stainless-steel grinding mill container with stainless steel balls in an EGOMA Auriga Planetary Ball Mill (India) at 500 rpm, under room temperature, and passed through an 80-mesh sieve to obtain an average particle size of smaller than 420 µ. The milled samples were kept separately in air-tight containers for several days at room temperature to proceed with the experiments. The raw, chopped, dried and milled samples are shown in Fig. 3.1.

Fig. 3.1. *S. spontaneum (Kans grass) (a), Banana (Musa spp.) Dwarf Cavendish (local name: "Jahaji") stem (b) peel (c) peduncle (d) their respective chopped and dried samples (a´, b´, c´, and d´), and respective milled samples (a´´, b´´, c´´, and d´´).*

3.2.3. Cellulose isolation from the untreated materials

The milled samples were subjected to chemical processing by soaking in NaOH (3%, w/w) solution for a period of 14 hours (fiber to liquid ratio 1:20). They were successively autoclaved in an SS-316 Mechomine Teflon lined-autoclave (India) under 137895 Pa (20 Psi) at a temperature of 210 ± 5°C, for a period of 45 min. The steam exploded samples were cooled to room temperature and then bleaching treatment was performed with a solution containing 5% H_2O_2 and pH 11.5 by adjusting with NaOH. Distilled water and ethanol were used to wash the substance after bleaching until neutral pH was obtained and dried at 80°C for 8 hours in a vacuum oven. The resulting product was acid hydrolyzed with 5% H_2SO_4 at a temperature of 50°C with an acid-to-material ratio of 1:15 for 2h (Taguchi design was used to optimize this step discussed in Section 3.3.3.). After hydrolysis, the cellulose was washed using distilled water to pH 7, and finally, a vacuum oven at 60°C for 5 hours at constant weight was used to dry the product. A schematic representation of the isolation procedure is provided in Fig. 3.2.

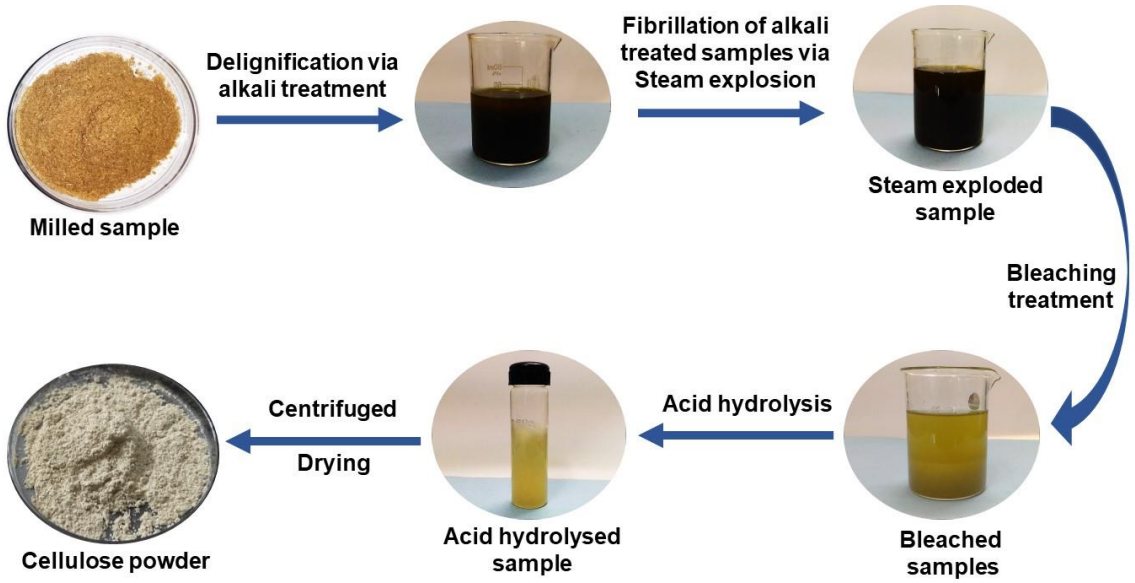

Fig. 3.2. *Schematic representation of the procedure for the extraction of cellulose [26].*

3.2.4. Optimizing acid hydrolysis variables using Taguchi design

The Taguchi experimental design is a distinctive and robust optimization technique that permits optimization with a minimum number of experiments [25]. This results in the reduction of time and cost for experimental investigations and enhances the performance characteristics. Keeping this in mind, we, therefore, choose the Taguchi design to investigate the effect of different hydrolysis parameters during the extraction of cellulose from the lignocellulosic samples. It is a statistical design of experiments technique based on orthogonal arrays. Unlike other traditional optimization techniques, where all the possible combinations are tested, Taguchi employs a set of minimum number of experiments that will provide complete data about all the influencing factors on the performance parameter. Thus, the method has the advantages of reducing the cost and the required time for experimental investigations and analyzing the effect of individual factors to predict the optimum condition. In this study, the factors: H_2SO_4 concentration, temperature, reaction time, and pulp-solution ratio were chosen. Each factor has three different levels (Table 3.1). In the full factorial design, four factors, at three levels each, would give 81 experiments (34). However, the L9 orthogonal array scheme of the Taguchi design gives only 9 experimental runs to complete the optimization process, as shown in Table 3.2.

Table 3.1. *Factors and their corresponding levels for the design of experimentations.*

Factors	Levels		
	1	2	3
(A) H_2SO_4 concentration (%)	5	10	25
(B) Reaction time (h)	2	5	8
(C) Temperature (°C)	50	80	120
(D) Pulp: solution ratio (g/ml)	1:15	1:20	1:50

Table 3.2. *L9 orthogonal array scheme of Taguchi design.*

Experiment	Abbreviation	Variables and Levels			
		A	B	C	D
1	Cellulose 1	1	1	1	1
2	Cellulose 2	1	2	2	2
3	Cellulose 3	1	3	3	3
4	Cellulose 4	2	1	2	3
5	Cellulose 5	2	2	3	1
6	Cellulose 6	2	3	1	2
7	Cellulose 7	3	1	3	2
8	Cellulose 8	3	2	1	3
9	Cellulose 9	3	3	2	1

3.2.5. Characterization

3.2.5.1. Chemical composition

The determination of the basic composition of raw material at each stage of treatment was conducted following the methods reported by the Technical Association of Pulp and Paper Industry (TAPPI). Determination of cellulose and hemicellulose contents was carried out according to TAPPI standard T203 OS-74 while the lignin content was determined according to TAPPI standard T222 OS-83. For each sample, three replicates were tested to obtain average values.

The moisture content of the samples at different stages of treatment was investigated by drying the samples in an oven for 24 h at 105°C. The weight of samples

before drying, W_i, and after drying, W_f were measured in order to determine the percentage moisture content using Eq. (1).

$$Moisture\ content = \frac{W_i - W_f}{W_f} \times 100 \quad (1)$$

The ash content of raw material and the subsequently treated samples were determined using thermogravimetric analysis data. The crucible containing the dried samples was placed in a muffle furnace and the temperature was raised from ambient temperature to 400°C at 20°C per min. The temperature was further raised to 575°C at 10°C per min and held for 10 h. The residual at this point can be attributed to ash.

3.2.5.2. Yield and Degree of Polymerization

The yield of prepared cellulose was calculated based on its weight over raw material and reported as a percentage. The weight of the final sample of cellulose, W_f, and the initial weight of raw material, W_i were measured in order to calculate the yield. Eq. (2) was used to determine the yield percentage.

$$Yield\ \% = \frac{W_f}{WI_i} \times 100 \quad (2)$$

The degree of polymerization was determined by the technique reported by Zhang et al. [29].

3.2.5.3. Microstructural characterizations

Fourier transform infrared (FTIR) spectroscopic study was used to detect possible changes in the functional groups existing in the samples at different stages of extraction. The spectra of the samples were obtained using a Perkin Elmer Spectrum 100 Optica FT-IR Spectrometer (USA). The samples were ground with Potassium Bromide (KBr) and pelletized with the help of a Qwik Handi-Press Kit. The IR spectra of the pellets were recorded at a wavelength range of 500–4000 cm^{-1} with 4 cm^{-1} resolution, for each sample. The X-ray diffractograms of the samples at different stages of extraction were obtained at room temperature within a 2θ range from 10° to 50° and a scan rate of 1° min^{-1} using the RIGAKU Miniflex Benchtop X-ray Diffractometer (Japan) with Ni filtered Cu Kα radiation (λ = 1.5406 Å) at the operating voltage 40 kV and current 15 mA. Before performing the XRD, all samples were dried at 50° C for 12 h in an air-circulating oven. The crystallinity index (CrI) of the material was determined using the equation

$$CrI = \frac{I_{200} - I_{am}}{I_{200}} \times 100$$

where CrI is the relative degree of crystallinity, I_{200} is the intensity of the 200-lattice diffraction at 2θ = 22.8°, and I_{am} is the intensity of diffraction at 2θ = 18°. I_{002} represents both crystalline and amorphous regions while I_{am} represents only the amorphous part.

The average hydrodynamic particle size of the cellulose samples in aqueous suspension was determined using the particle size analyzer Zetasizer Nano-ZS-90 (Malvern Instruments, UK) operating at a wavelength of 633 nm and a scattering angle of 90°, under a constant temperature of -25°C.

3.2.5.4. Thermogravimetric analysis (TGA)

The thermal stability of the raw sample and the samples at different stages of extraction were comparatively estimated by TGA (Thermogravimetric Analysis) measurements performed using an STA 6000 Simultaneous Thermal Analyzer from Perkin Elmer (USA). All the spectra were recorded under an ambient nitrogen atmosphere by gradual heating of the samples from room temperature to 700 ºC at a heating rate of 20 ºC min^{-1}.

3.2.5.5. Morphological analysis

A scanning electron microscope model JEOL JSM-6390 with an accelerating voltage of 10–20 kV was employed to observe the surface morphology of the samples at different stages of treatment. Prior to the SEM examination, the samples were oven-dried at 60°C for 8 h and then a fine layer of gold was deposited on the samples by means of a plasma sputtering apparatus to avoid charging.

3.3. Results and discussion

3.3.1. Isolation of cellulose and chemical composition

Cellulose was derived from *S. spontaneum*, banana pseudostem, banana peel, and banana peduncle through the integrated treatment of alkali and steam explosion methods followed by bleaching and acid hydrolysis. The isolation procedure is a significantly quicker, economical, and environmentally sustainable method, wherein the bleaching step was executed by an entirely chlorine-free method. Also, the steam explosion step was performed only for 45 mins while the acid hydrolysis process has been thoroughly optimized and used low concentration sulfuric acid.

The chemical analysis of native samples and their forms at different stages of treatment was carried out in order to estimate the percentage of components present in the samples. The comparative chemical composition of the different samples is presented in Table 3.3. The native *S. spontaneum* consists of 48.23% cellulose, 32.01% hemicellulose, 17.09% lignin, 2.67% ash, and 1.43% moisture content. Upon NaOH treatment and steam explosion, the cellulose content in the residual mass was enriched to 61.14%, whereas the hemicellulose content was reduced to 8.4%. Similarly, the raw banana pseudostem consists of 49.12% cellulose, 36.09% hemicellulose, 8.22% lignin, 3.37% ash, and 3.1% moisture content. The cellulose content in the residual mass was enhanced to 59.10% after alkali treatment and steam explosion, while the hemicellulose was reduced to 19%. Likewise, the cellulose content in the raw banana peel and raw banana peduncle was 43.22% and 63.12%, respectively which upon treatment with alkali and steam explosion increases to 58% and 68.55%, respectively. On the other hand, reduction of hemicellulose content from 28.12% to 16.45% and from 21.71% to 11.13% was observed in the case of banana peel and banana peduncle, respectively. The large reduction in hemicellulose was caused by the simultaneous alkaline treatment and steam explosion, where the alkali treatment solubilized hemicellulose, while the steam explosion caused a substantial breakdown of the lignocellulosic secondary structures that led to improved defibration. During the steam explosion, partial hydrolysis of the hemicellulose fraction and depolymerization of the lignin component also takes place resulting in water-soluble sugars and phenolic compounds. Accordingly, the alkali-treated fiber when subjected to steam explosion the remaining hemicellulose fraction after alkali treatment, and some percentage of the lignin components dissolves. Hence a decrease in lignin fraction from 17.09% to 12.64% was observed in the case of *S. spontaneum* and from 8.22% to 3.82%, 24.1% to 11.34%, and 14.3% to 3.69% in the case of banana pseudostem, peel, and peduncle, respectively. The steam exploded fibers were then subjected to bleaching treatment aiming for the removal of lignin. Lignin is linked with the carbohydrate moiety through alkali-sensitive linkage or ether-type linkage between lignin hydroxyl groups and hydroxyls of cellulose. Degradation of lignin forms hydroxyl, carbonyl, and carboxylic groups that help in solubilizing the lignin content in the alkali medium, thereby facilitating the purification of cellulose [30]. After the bleaching treatment, lignin content was reduced from 12.64% to 0.27% for *S. spontaneum*, 3.82% to 0.38% for banana pseudostem, from 11.34% to 0.28% for banana peel, and from 3.69% to 0.27% for banana peduncle. To summarize, the

chemical analysis data (Table 3.3) shows that the cellulose content enriched from 48.23% in the native *S. spontaneum* to 83.33% in the derived cellulose, whereas the net hemicellulose and lignin contents decreased from 32.01% to 1.42% and 17.09% to 0.27%, respectively. Similar results showing increased cellulosic content and decreased hemicellulose and lignin have been observed in the case of banana peel and pseudostem (Table 3.3). In comparison, Adel et al. when using bleaching accompanied by acid hydrolysis, alone attained a cellulose enrichment yield of ~72.3%, when isolating cellulose from rice hulls using 5% H_2SO_4 and 10% NaClO [31]. Other studies have reported that acid-alkaline or alkaline-acid treatment followed by chlorination and bleaching can produce 66.2% - 64.7%, 59.8%, and 77.11% yields of cellulose from rice straw, coconut fiber, and pine residual sawdust respectively [32, 33, 34]. These yields happen to be lower than the cellulose yields obtained from *S. spontaneum* and banana agrowastes in the present study (Table 3.5). Fig. 3.3 a represents the comparison of the chemical composition of *S. spontaneum*, banana pseudostem, peel, and peduncle used in this study compared to other reports, while Fig. 3.3 b represents their respective chemical composition obtained after different pretreatments.

It is worth observing that cellulose when extracted using traditional methods, has higher residual lignin content if chlorine-based compounds are used for bleaching [32, 38]. The quality of cellulose yield in this study using the integrated approach has been promising as can be seen from Fig. 3.3.

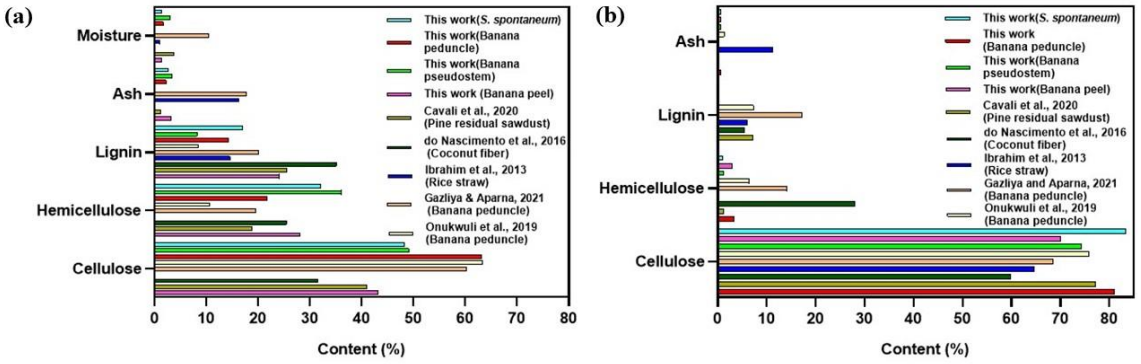

(c)

Composition	This work (*S. spontaneum*)		This work (Banana peduncle)		This work (Banana pseudostem)		This work (Banana peel)		[34] (Pine residual sawdust)		[33] (Coconut fiber)		[32] (Rice straw)		[35] (Banana peduncle)		[36] (Banana peduncle)	
	Raw (%)	Pretreated (%)	Raw (%)	Pretreated (%)	Raw (%)	Pretreated (%)	Raw (%)	Pretreated (%)	Raw (%)	Pretreated (%)	Raw (%)	Pretreated (%)	Raw (%)	Pretreated (%)	Raw (%)	Pretreated (%)	Raw (%)	Pretreated (%)
Cellulose	48.23	83.33	63.12	81	49.12	74.32	43.22	70.14	41	77.11	31.6	59.8		64.7	60.35	68.55	63.4	75.81
Hemicellulose	32.01	0.96	21.71	3.41	36.09	1.29	28.12	2.96	18.89	1.21	25.5	28			19.54	14.12	10.56	6.45
Lignin	17.09	0.07	14.3	0.06	8.22	0.05	24.1	0.07	25.54	7.19	35.1	5.5	14.6	6.1	20.11	17.33	8.5	7.31
Ash	2.67	0.72	2.19	0.64	3.37	0.62	3.13	0.67	1.16				16.3	11.3	17.82			1.34
Moisture	1.43		1.68		3.1		1.43		3.75				1		10.52			

Fig. 3.3. *Comparison of the native lignocellulosic content in various feedstocks w.r.t. S. spontaneum and banana agrowastes (this work) (a); cellulose recovery and lignocellulosic residues after cellulose isolation using the ammonia/chlorine-free, mild acid-treated integrated approach (S. spontaneum, banana peduncle, pseudostem, peel) (this work), 5% H_2SO_4 treatment at 170°C (pine residual sawdust), alkaline-acid treatment followed by chlorination and bleaching (coconut fiber and rice straw), microwave-assisted alkaline delignification (banana peduncle) and acetylation treatment containing 60% H_2SO_4 (banana peduncle) (b); comparative table representing the percentage composition of lignocellulosic components before and after cellulose extraction (c) [37].*

Table 3.3. *Chemical composition of the primary constituents of S. spontaneum, banana pseudostem, banana peel, and banana peduncle at different stages of treatment.*

Sample	Cellulose (%)	Hemicellulose (%)	Lignin (%)	Ash (%)	Moisture content (%)
S. spontaneum	48.23 ± 1.9a	32.01 ± 1.35	17.09 ± 0.60	2.67 ± 0.42	1.43 ± 0.76
Alkali treated	61.14 ± 1.1	8.4 ± 0.80	12.64 ± 0.78	1.01 ± 0.33	0.76 ± 0.50
Bleached	75 ± 0.54	1.42 ± 0.48	0.27 ± 0.57	0.77 ± 0.21	0.44 ± 0.35
Cellulose	83.33 ± 0.47	0.96 ± 0.31	0.07 ± 0.25	0.72 ± 0.10	-
Banana pseudostem	49.12 ± 1.7	36.09 ± 1.43	8.22 ± 0.40	3.37 ± 0.62	3.1 ± 0.46
Alkali treated	59.10 ± 0.86	19 ± 0.98	3.82 ± 0.56	1.72 ± 0.45	0.94 ± 0.34
Bleached	66.69 ± 0.44	3.74 ± 0.23	0.38 ± 0.30	0.76 ± 0.34	0.41 ± 0.12
Cellulose	74.32 ± 0.23	1.29 ± 0.31	0.05 ± 0.22	0.62 ± 0.18	-

Banana peel	43.22 ± 1.33	28.12 ± 1.25	24.1 ± 0.67	3.13 ± 0.42	1.43 ± 0.59
Alkali treated	58 ± 1.10	16.45 ± 0.98	11.34 ± 0.39	2 ± 0.01	0.4 ± 0.08
Bleached	61.29 ± 0.62	11.12 ± 0.53	0.28 ± 0.16	0.75 ± 0.22	0.35 ± 0.23
Cellulose	70.14 ± 0.44	2.96 ± 0.31	0.07 ± 0.21	0.67 ± 0.21	-
Banana peduncle	63.12 ± 1.56	21.71 ± 1.91	14.30 ± 0.72	2.19 ± 0.44	1.68 ± 0.84
Alkali treated	68.55 ± 0.91	11.13 ± 0.75	3.69 ± 0.91	1.7 ± 0.28	0.84 ± 0.50
Bleached	70.67 ± 0.55	10.32 ± 0.47	0.27 ± 0.69	0.8 ± 0.21	0.45 ± 0.27
Cellulose	81 ± 0.34	3.41 ± 0.29	0.06 ± 0.36	0.64 ± 0.11	-

3.3.2. FTIR spectroscopy analysis

Different stages of chemical treatment on the four raw materials were studied using FTIR spectroscopy. The comparative FTIR spectra of raw samples with that of alkali-treated, bleached, and the final cellulose obtained are shown in Fig. 3.4 a, b, c, and d for *S. spontaneum*, banana pseudostem, banana peel, and banana peduncle, respectively. The fingerprints of the functional groups for different stages are labeled in the figures. The absorption band at around 3404-3417 cm^{-1} observed in all the spectra, is ascribed to the stretching of O-H groups present in cellulose, hemicellulose, and lignin [39]. The band observed at ~1733 cm^{-1} in the FTIR spectra of all the raw samples and the alkali-treated samples are attributed to either C=O stretching of the acetyl and uronic ester groups of hemicellulose or the ester linkage of carboxylic groups of p-coumaric and ferulic acids of lignin and/or xylan in hemicellulose [40]. Whereas this band is no longer present in the bleached spectra and the extracted cellulose spectra. The cleavage of the ester linkages of hemicellulose and lignin upon alkali treatment and successive bleaching could explain the absence of the C=O stretching band. This was supported by the findings of the chemical composition study (Table 3.3), which confirmed that the bleaching procedure reduced lignin levels to negligible. The C=C stretching of the aromatic skeletal vibrations of the functional groups of lignin is responsible for the band observed at ~1517 cm^{-1} [41]. The band at 1264 cm^{-1}, on the other hand, is caused by a weak C-O stretch of pectic acid that is most likely present. These two peaks disappeared after the bleaching treatment, indicating that lignin was effectively eliminated. Due to the presence of strong cellulose water interaction and the stretching of C-H groups, the absorption bands at around 1628-

1642 cm^{-1} and 2905-2934 cm^{-1} in all the spectra were correlated with the stretching vibration of O-H groups of absorbed water [42]. Bands around 1041-1067 cm^{-1}, 1341-1384 $cm^{-1,}$ and 1432-1446 cm^{-1} were allocated to the skeletal vibration of the C-O-C pyranose ring present in cellulose, bending C-H vibration, and CH_2 bending vibration, respectively [43]. Lastly, the diagnostic band at 897 cm^{-1} is attributed to the β-glycosidic linkage vibration in cellulose which is apparent in all the spectra [44].

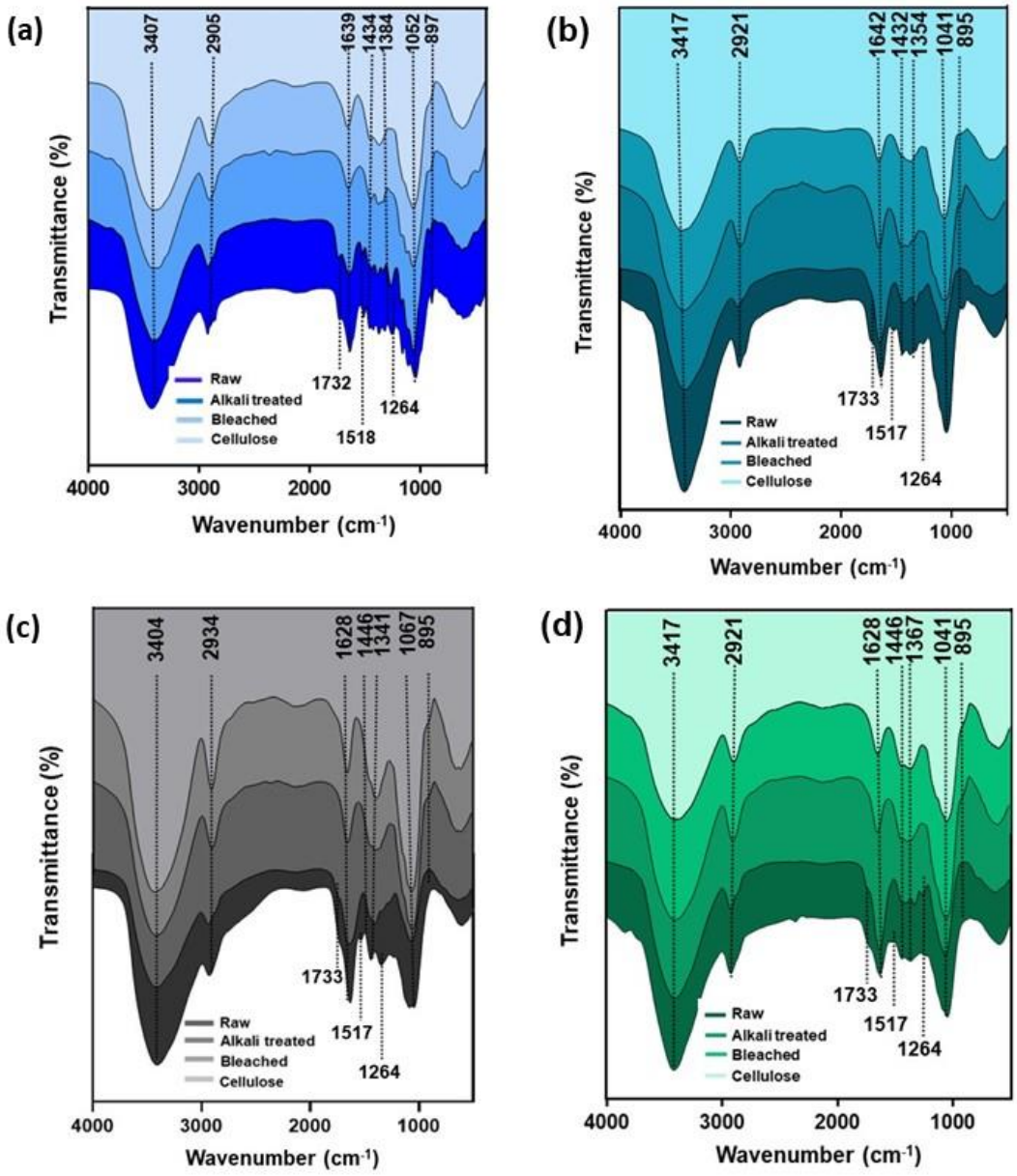

Fig. 3.4. *FTIR spectra of S. spontaneum (a), banana pseudostem (b), banana peel (c), and banana peduncle (d) at different stages of treatment.*

3.3.3. X-ray diffraction analysis

Comparative XRD studies were performed to explore the crystalline structure of the samples at their different stages of treatment. The XRD patterns of the raw, alkali-treated, bleached, and final cellulose obtained are presented in Fig. 3.5 a, b, c, and d for *S. spontaneum*, banana pseudostem, banana peel, and banana peduncle, respectively.

All the X-ray diffraction spectra of *S. spontaneum* (Fig. 3.5 a) display three well-defined crystalline peaks at $2\theta = 14.8^{\circ}$, 16.5° and 22.6° which corresponds to the crystal planes $(1\bar{1}0)$, (110), and (200), respectively, and is in close agreement with the theoretical values. The spectra of bleached *S. spontaneum* and derived cellulose display doublet crystalline peaks at around $2\theta = 22.6^{\circ}$, which was associated with the presence of two polymorphs of cellulose I (peak $2\theta = 22.6^{\circ}$) and cellulose II (peak $2\theta = 22$) [45]. Similarly, the diffraction patterns of all the spectra of banana pseudostem (Fig. 3.5 b) and banana peduncle (Fig. 3.5 d) displayed characteristic cellulose I crystalline structure with peaks at $2\theta = 22.2°$ and 15.5°, conforming to (200) and (110) plane sites, respectively [46]. These results agree with previous reports, where cellulose extracted from banana pseudostem was observed [47]. According to Flores-Jerónimo et al. [48], the crystallinity of cellulose increases with increased hydrogen bonding interactions and van der Waals forces between adjacent molecules. In contrast, banana peel (Fig. 3.5 c) showed distinctive peaks around 12.6° (101) and 21° (200), owing to the crystallographic plane of type I cellulose [49].

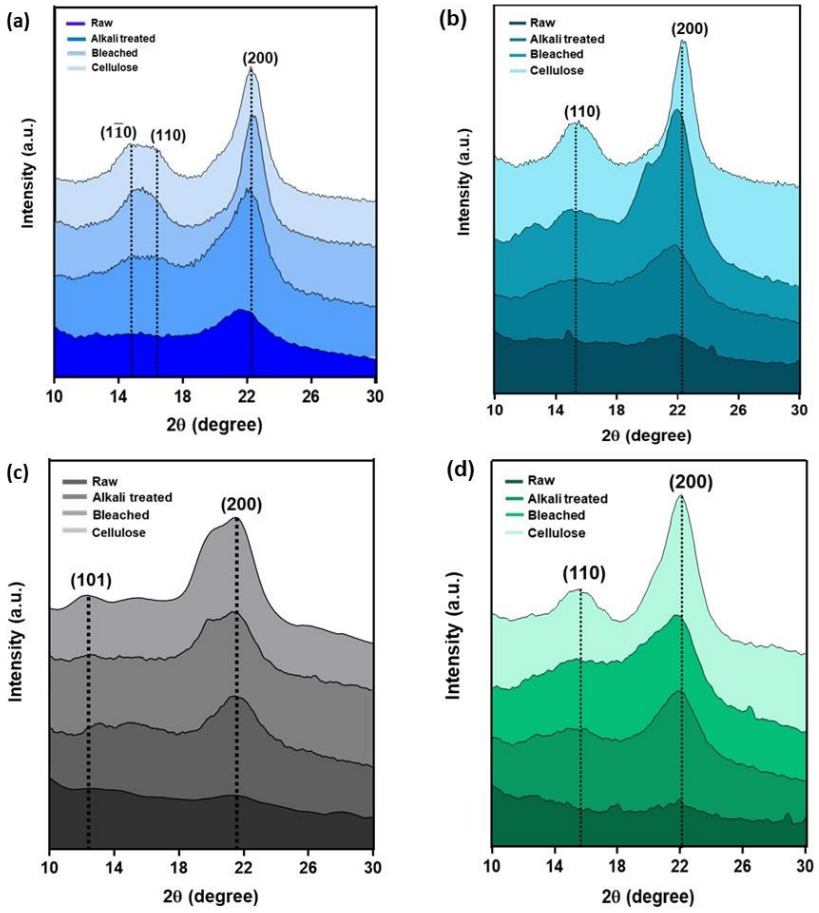

Fig. 3.5. *XRD spectra of S. spontaneum (a), banana pseudostem (b), banana peel (c), and banana peduncle (d) at different stages of treatment.*

The crystallinity index (CrI) for the various samples is presented in Table 3.4. The crystallinity indices of raw, alkali-treated, bleached, and cellulose obtained from *S. spontaneum* were found to be 32.90%, 50.70%, 68.81%, and 74.06%, respectively, for banana pseudostem, it was 20.76%, 26.74%, 38.55%, and 56.21% and for banana peel, it was 19.9%, 25.56%, 35.43%, and 58.60%, respectively. For banana peduncle, the indices are 21.96%, 27.84%, 36.53%, and 65.32% corresponding to raw, alkali-treated, bleached, and final cellulose obtained after acid hydrolysis. These findings clearly show that the crystallinity of the samples increases with each successive chemical treatment. This can be seen from Fig. 3.5 a, b, c, and d that the peak at 2θ ~22° is sharper for the chemically treated sample than the raw ones. The high CrI value of the chemically treated samples relative to the raw samples is due to the degradation of amorphous hemicellulose and the delignification process caused by the alkaline, bleaching, and acid hydrolysis treatments which result in the enrichment of cellulose in the residues [50]. Furthermore, dissolved inorganic compounds may also aid in the exposure of crystalline cellulose in the residues.

Table 3.4. *Crystallinity index (CrI) value of S. spontaneum (a), banana pseudostem (b), banana peel (c), and banana peduncle (d) at different stages of treatment.*

Sample	Crystallinity index (CrI)			
	Raw	**Alkali treated**	**Bleached**	**Cellulose**
S. spontaneum	32.9 %	50.7 %	68.81 %	74.06 %
Banana pseudostem	20.76 %	26.74 %	38.55 %	56.21 %
Banana peel	19.9 %	25.56 %	35.43 %	58.60 %
Banana peduncle	21.96 %	27.84 %	36.53 %	65.32 %

3.3.4. Thermogravimetric analysis (TGA)

The thermal stability of untreated samples and their forms at various steps is shown by thermogravimetric analysis (TGA) (Fig. 3.6 a, d, g, and j) and derivative thermogram (DTG) (Fig. 3.6 b, e, h, and k) and the data of thermal analysis are presented in Fig. 3.6 c, f, i, and l, respectively. The weight reduction procedures for all the samples can be separated into three major phases (Fig. 3.6 a, d, g, and j). The first stage (60°C - 150°C) is attributed to the primary weight loss induced by water volatilization or low-molecular-weight compounds. Cellulose decomposition temperature in raw *S. spontaneum*, pseudostem, peel, and peduncle begins at 233°C, 200°C, 257°C, and 203°C, respectively, while in their isolated cellulose it begins at 293°C, 306°C, 306°C, and 293°C, respectively. The degradation peak temperature of raw *S. spontaneum*, pseudostem, peel, and peduncle occurs at 262°C, 219°C, 271°C, and 225°C, respectively, which gradually increases in each case as a result of sequential chemical treatments as presented in Fig. 3.6 c, f, i, and l. For *S. spontaneum* the highest degradation peak temperature of isolated cellulose is 338°C, while for banana peduncle, it is 325°C. The degradation of cellulosic components for all the materials continues up to 380°C, when the cellulose and hemicellulose fractions decompose, depolymerize, and decarboxylate. In the range of 400–700°C, aromatization, lignin pyrolysis, and combustion occurred, resulting in char residues [51].

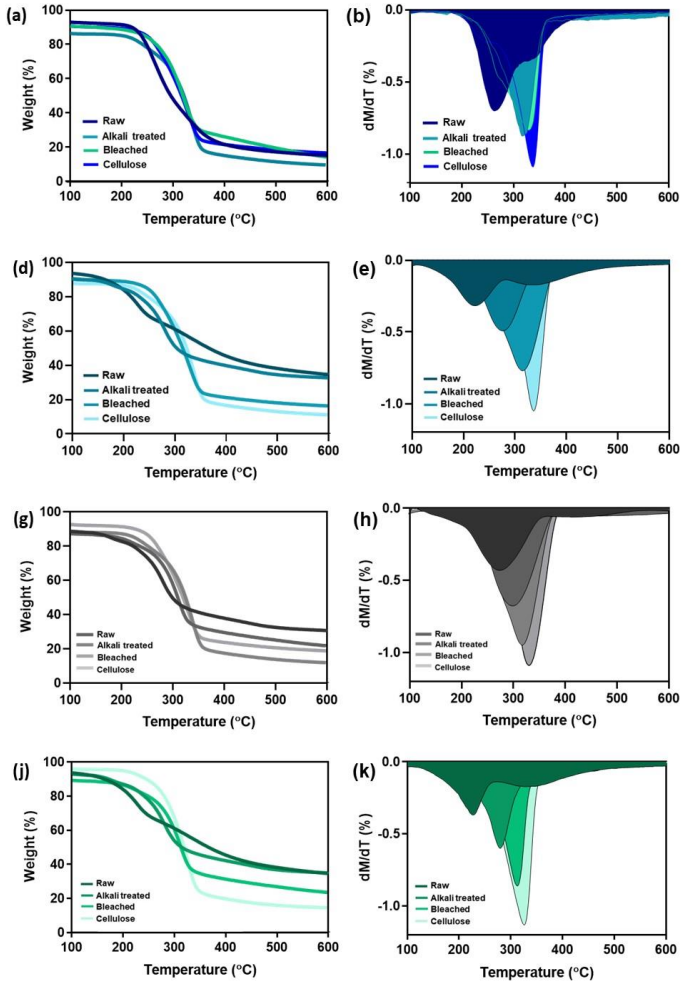

(c)

Sample	*Saccharum spontaneum*			
	$T_{initial}$ (°C)[#]	T_{peak} (°C)[*]	W_{loss} (%)[©]	$W_{residue}$ (%)[µ]
Raw	233	262	78.5	15.3
Alkali treated	264	312	78.7	13.3
Bleached	266	330	76.7	12
Cellulose	292	338	80	7.67

(f)

Sample	Banana pseudostem			
	$T_{initial}$ (°C)[#]	T_{peak} (°C)[*]	W_{loss} (%)[©]	$W_{residue}$ (%)[µ]
Raw	200	219	55.33	34.67
Alkali treated	255	275	56.91	30.5
Bleached	282	314	72.92	16.67
Cellulose	306	332	75.91	8.75

(i)

Sample	Banana peel			
	$T_{initial}$ (°C)[#]	T_{peak} (°C)[*]	W_{loss} (%)[©]	$W_{residue}$ (%)[µ]
Raw	257	271	56.92	30.75
Alkali treated	283	298	64.09	23.08
Bleached	296	316	72.92	16.67
Cellulose	306	320	75	10.17

(l)

Sample	Banana peduncle			
	$T_{initial}$ (°C)[#]	T_{peak} (°C)[*]	W_{loss} (%)[©]	$W_{residue}$ (%)[µ]
Raw	203	225	48.92	34.25
Alkali treated	251	278	54.92	30.5
Bleached	281	310	63.42	22.92
Cellulose	293	325	80.33	15.25

Fig. 3.6. *TGA curves (a, d, g, j), DTG curves (b, e, h, k), and thermal analysis data (c, f, i, l) of S. spontaneum, banana pseudostem, banana peel, and banana peduncle at various phases of treatment.* [#]*TGA initial decomposition temperature,* [*]*DTG peak temperature,* [©]*TGA maximum weight loss,* [µ]*TGA char residue weight.*

Moreover, the isolated cellulose tends to lose weight at temperatures higher than the untreated samples, owing to its high purity. The char residue levels at 400–700°C in the untreated samples were unusually high, ranging from 30–35% as shown in Fig. 3.6 c, f, i, and l. This was seen to reduce to 8–15%, following the successive pretreatments for the respective isolated celluloses.

The maximum degradation peak temperature value of the *S. spontaneum* extracted cellulose is comparable to that of cellulose obtained from roselle fibers (340°C) where the sodium hypochlorite bleaching step is followed by 8% NaOH treatment and 2.5 M HCl hydrolysis [44]. Likewise, comparable thermograms have been reported for cellulose fibers extracted from banana peel using microwave digestion method and ball milling assisted ultra-sonication method, as well as cellulose fibers extracted from banana

pseudostem using a combination of bleaching (6% of sodium chlorite solution) and liquefaction processes [mixed solvent of PEG400, glycerine, and H_2SO_4 (98%, 1 mmol/g of substrate)] [46, 49]. The isolated cellulose has a maximal degradation peak temperature range of 320-332°C, equivalent to celluloses derived from tucumã's endocarp (332°C), which used a chlorine-based bleaching step (2.5% sodium hypochlorite) overnight after delignification was done at 135°C using an autoclave and 20% NaOH for 30 min [52] and cellulose extracted from oil palm empty fruit branches (325°C) using formic acid and 10% of H_2O_2 at 85°C (Table 3.5) [53].

Table 3.5. *A comparison of the different alkaline, bleaching, and hydrolysis conditions for obtaining cellulose with diverse yields, crystallinity index, and thermal stabilities from reported studies.*

Lignocellulosic sources	Alkaline treatment	Bleaching step	Acid hydrolysis	Yield (%)	CrI (%)	T_{peak} (°C)	References
S. spontaneum	3% NaOH	5% H_2O_2	5% H_2SO_4	83	74.06	338	This work
Banana peduncle	3% NaOH	5% H_2O_2	5% H_2SO_4	81	65.32	325	This work
Rice straw	10% NaOH	60% NaOCl	5% H_2SO_4	64.7	66.7	301	[32]
Coconut fiber	3.8% NaOH	5% H_2O_2	44% H_2SO_4	59.8	68	300	[33]
Pine residual sawdust	10% NaOH	Not mentioned	5% H_2SO_4	77.11	Not mentioned	Not mentioned	[34]
Banana pseudostem	12% NaOH	6% $NaClO_2$	Not mentioned	Not mentioned	77.13	316	[49]
Tucumã's endocarp	20% NaOH	2.5% NaOCl	Not mentioned	Not mentioned	48.5	333	[52]
Oil Palm Fruit Bunches	Not mentioned	10% H_2O_2	20% HCHOOH	64	69.9	325	[53]
Rice husk	5% NaOH	5% H_2O_2	5% H2SO4+25% CH_3COOH	63.38	72.88	347	[54]
Rice husk	5% NaOH	5% H_2O_2	10% HNO_3+25% CH_3COOH	65.51	79.29	339	[54]
Sugarcane bagasse	10% NaOH	Not mentioned	70% HNO_3+80% CH_3COOH	43.6	Not mentioned	320	[55]

3.3.5. Morphological analysis

SEM graphs of the raw samples exhibit an irregular plane with uneven flaky assemblies and the clusters are supposed to be made up of hemicellulose, lignin, and other non-cellulosic components (Fig. 3.7). Post alkali treatment, the surface becomes grainier and coarser, indicating further extrusion of the peripheral non-cellulosic like hemicelluloses,

lignin, wax, pectin, and other impurities. The bleached samples have even, clear, and small rod-like images, indicating near-complete elimination of hemicellulose and lignin. This result indicates that the alkaline treatment alone is insufficient to strip all non-cellulosic elements and is supported by FTIR spectra (Fig. 3.4. a, b, c, and d). Cellulose obtained after acid hydrolysis have a more uniform fiber-like morphology with random orientation which was likely to be induced by the H_2SO_4 solution penetrating the amorphous areas of cellulose and disintegrating the β-1, 4-glycosidic bonding between the repeating units [48].

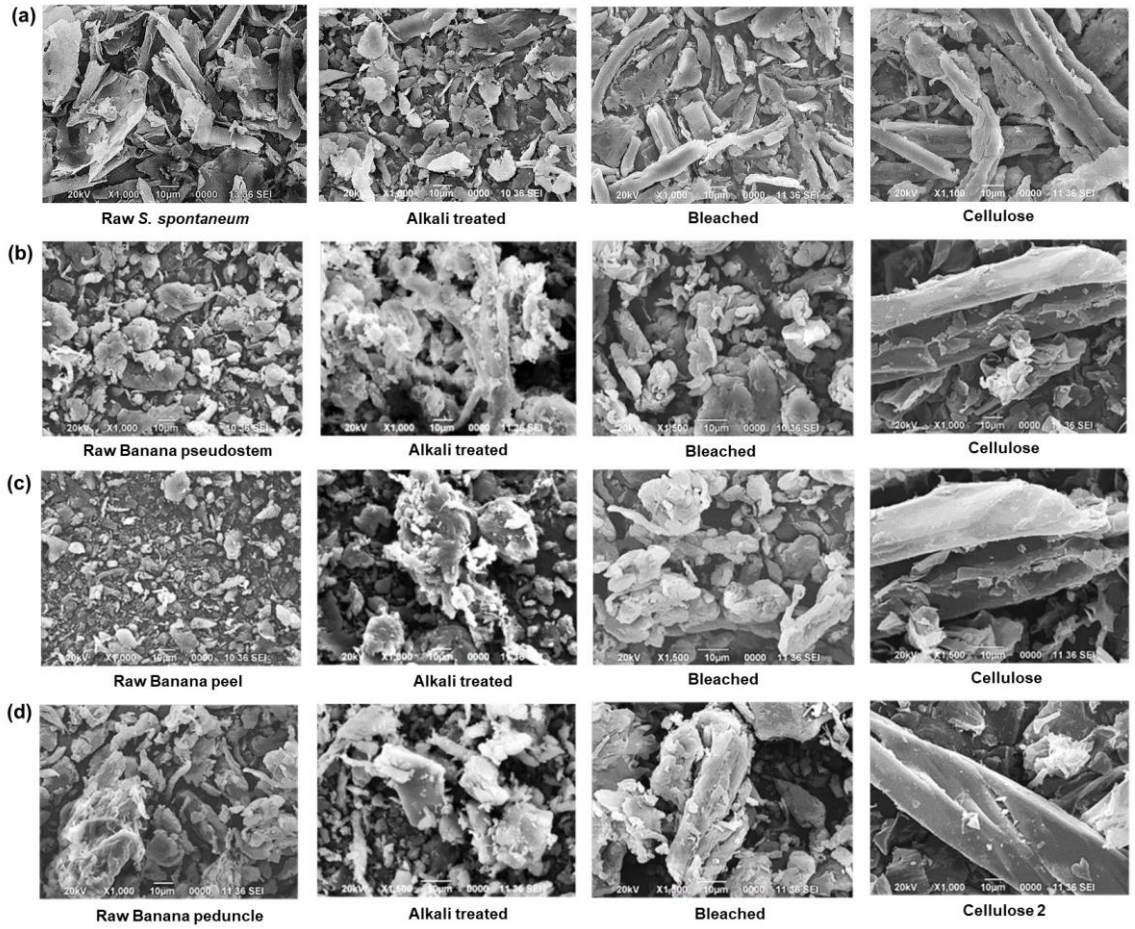

Fig. 3.7. *SEM images of S. spontaneum (a), banana pseudostem (b), banana peel (c), and banana peduncle (d) at different stages of pretreatment.*

3.3.6. Optimization of acid hydrolysis treatment using Taguchi design

The comparative analysis of the structure, crystallinity, and thermal stability of the raw samples, alkali-treated, bleached, and cellulose obtained after acid hydrolysis established the entire extraction process from the chosen lignocellulosic biomasses. However, the

physico-chemical properties of the isolated cellulose greatly depend on the acid hydrolysis process parameters. Hence, the objective was to optimize the hydrolysis conditions for obtaining high-quality pure cellulose with the highest yield and lowest degree of polymerization (DP) using minimal acid concentrations, to keep the process environment friendly. An ammonia/chlorine-free bleaching step was introduced subsequently to support the sustainability aspect. Banana peduncle yielding the highest recovery of cellulose among the three banana agrowastes was proceeded for further optimization of acid hydrolysis, applying Taguchi design. Accordingly, the nine experimental runs obtained (Table 3.2) from the Taguchi design were tested for each source (*S. spontaneum* and banana peduncle) separately to attain high-quality cellulose by optimizing hydrolysis conditions.

The highest yield of cellulose obtained from *S. spontaneum* was found to be 83% under Cellulose 1 conditions after 120 min of hydrolysis treatment with 5% H_2SO_4 concentration at 50°C in a 1:15 pulp-solution ratio (Table 3.6). In the case of banana peduncle, the maximum yield of cellulose produced was determined to be 81% under Cellulose 2 conditions after 5 h of hydrolysis using 5% H_2SO_4 at 80°C in a 1:20 pulp-solution ratio (Table 3.7). This could be accomplished due to the optimized pulp-solution ratio, under effective low acid pre-treatment conditions and are in agreement with previous reports for cellulose extraction from banana pseudostem using low acid concentrations [47]. Two recent studies on acid hydrolysis of rice husk using a solution comprising 5% H_2SO_4, 5% H_2O_2, and 25% CH_3COOH yielded 63.38% cellulose while another using 10% HNO_3, 5% H_2O_2, and 25% CH_3COOH reported only 65.51% cellulose yield [54]. The yield in the current study is also greater than cellulose yields (43.6% and 43%) from sugarcane bagasse using 70% nitric acid and 80% acetic acid [55] and the orange peel extracted celluloses (40.4% and 45.2%), using sodium sulfite and sodium metabisulfite digestions [56]. The differences in the yield gained are also highly dependent on the source sample in addition to the hydrolysis conditions.

The degree of polymerization is an important factor to consider when assessing the impact of acid hydrolysis on cellulose chains. The degree of polymerization (DP) and viscosity-average molecular weight (M_w) was determined using an intrinsic viscosity measurement. The DP values and the M_w of the 9 cellulose samples obtained in each study of *S. spontaneum* and banana peduncle are shown in Table 3.6 and Table 3.7. Since the hydrolysis of cellulose depolymerizes the cellulose chains, lower DP levels offer more

binding sites for cellulases, boosting the rate of downstream hydrolysis [57]. From Table 3.6, it is seen that the DP of the cellulose sample obtained under the acid hydrolysis condition: 5% H_2SO_4, reaction time (2h), temperature (50°C), and pulp to solution ratio (1:15), has the lowest value (101) which was almost similar to the DP (101.6) of cellulose nanofibers isolated from curaua fibers [58] and lower than that of sugar beet pulp (120) [59]. Similarly, the DP of the highest yielding peduncle cellulose variant, cellulose 2 has a low DP value of 155, as seen in Fig. 5b. This is significantly lower than celluloses recovered from varied feedstocks like oil palm empty fruit branch (500) [60], sugar palm (946) [41], sugarcane bagasse (822) [55], and orange peel (344) [56].

Table 3.6. *Yield, molecular weight (M_w), and degree of polymerization (DP) of nine (09) cellulose samples obtained from S. spontaneum under different hydrolysis conditions.*

Experiment	Variables and levels				Yield[a] (%)	M_w[a] (g/mol)	DP[a]
	A	B	C	D			
Cellulose 1	**1**	**1**	**1**	**1**	**83 ± 1.08[b]**	**16472 ± 0.16**	**101 ± 0.20**
Cellulose 2	1	2	2	2	81 ± 1.05	33924 ± 0.34	209 ± 0.42
Cellulose 3	1	3	3	3	82 ± 1.07	25066 ± 0.25	155 ± 0.31
Cellulose 4	2	1	2	3	78 ± 1.01	57100 ± 0.57	352 ± 0.70
Cellulose 5	2	2	3	1	65 ± 0.85	39713 ± 0.40	245 ± 0.49
Cellulose 6	2	3	1	2	80 ± 1.04	28323 ± 0.28	175 ± 0.35
Cellulose 7	3	1	3	2	67 ± 0.87	28952 ± 0.29	179 ± 0.36
Cellulose 8	3	2	1	3	72 ± 0.94	67559 ± 0.68	417 ± 0.83
Cellulose 9	3	3	2	1	76 ± 0.98	176512 ± 1.77	1090 ± 2.18

[a] Values are Mean ± SD of triplicate analysis.

Table 3.7. *Yield, molecular weight (M_w), and degree of polymerization (DP) of nine (09) cellulose samples obtained from banana peduncle under different hydrolysis conditions.*

Experiment	Variables and levels				Yield[b] (%)	M_w[b] (g/mol)	DP[b]
	A	**B**	**C**	**D**			
Cellulose 1	1	1	1	1	79 ± 0.94	30843 ± 0.45	165 ± 0.70
Cellulose 2	**1**	**2**	**2**	**2**	**81 ± 0.97**	**19583 ± 0.26**	155 ± 0.43
Cellulose 3	1	3	3	3	76 ± 1.03	36278 ± 0.65	205 ± 0.56
Cellulose 4	2	1	2	3	71 ± 1.11	74324 ± 0.83	402 ± 0.87

Cellulose 5	2	2	3	1	69 ± 0.94	50967 ± 0.71	365 ± 0.73
Cellulose 6	2	3	1	2	73 ± 0.91	36798 ± 0.37	230 ± 0.43
Cellulose 7	3	1	3	2	65 ± 1.13	36734 ± 0.48	235 ± 1.68
Cellulose 8	3	2	1	3	70 ± 1.08	81222 ± 0.97	575 ± 1.20
Cellulose 9	3	3	2	1	67 ± 1.21	99769 ± 0.89	605 ± 0.95

[b] Values are Mean ± SD of triplicate analysis.

X-ray diffractograms of the 9 cellulose samples obtained from *S. spontaneum* and banana peduncle under different hydrolysis conditions are shown in Fig. 3.8 a and Fig. 3.8 b, respectively. In order to compare the crystallinity of the 9 variants of each source, the crystallinity index (CrI) values, interplanar distance (d-spacing) for each crystallographic plane, and crystallite size perpendicular to each of the three planes (L) is presented in Table 3.8 and Table 3.9. The crystal planes ($1\bar{1}0$), (110), and (200) are noted with the indexes 1, 2, and 3, respectively. The d-spacing values are indicative of the changes in the type of cellulose polymorphs (I and II), while the crystallite size (L) represents the material stiffness. It is clear from the table that, after acid hydrolysis, d-spacing data of the crystal surfaces do not vary considerably. Meanwhile, the effect of acid hydrolysis conditions on the crystallite sizes were presented in Table 3.8 and Table 3.9. A correlation was observed between the L2 values of the crystal plane (110) and the crystallinity index values of the cellulose samples. This is attributed to the fact that the (110) plane contains more –OH groups and is, therefore, more liable to be influenced by the acid hydrolysis process. In general, the lower the value of L2, the higher the value of CrI. The highest CrI value in the case of *S. spontaneum* was obtained for Cellulose 1 (74.06%), where the acid hydrolysis conditions were 5% H_2SO_4, reaction time (2h), temperature (50°C), and pulp to solution ratio (1:15). However, with an increase in reaction time and temperature, the crystallite sizes increase and CrI value decreases as evident from Cellulose 2 (73.96%) and Cellulose 3 (69.69%). This can be related to the degradation of crystalline cellulose with an increase in reaction time and temperature. On the other hand, the increase in the CrI values for Cellulose 4 (71.44%) compared to Cellulose 3 (69.69%) and Cellulose 7 (69.94%) compared to Cellulose 5 (69.69%) and Cellulose 6 (67.33%) can be justified with the fact that although these conditions were carried out with higher acid concentrations, the reaction time was relatively shorter than that for Cellulose 7 conditions and also lower reaction temperature in case of Cellulose 4 conditions. A similar observation was found in

the case of banana peduncle, where, Cellulose 2 (65.32%) had the maximum CrI value, with acid hydrolysis conditions of 5% H_2SO_4, temperature (80°C), reaction duration (5h), and pulp-solution ratio (1:20). Nonetheless, as the temperature and reaction duration are increased, crystallite sizes grow larger and the CrI value declines, as seen in Cellulose 3 (64.62%), Cellulose 5 (63.83%), and Cellulose 9 (63.40%). In contrast, the rise in CrI values of Cellulose 1 (64.66%) compared to Cellulose 3 (64.62%), Cellulose 4 (64%) compared to Cellulose 6 (63.57%), and Cellulose 7 (63.71%) compared to Cellulose 9 (63.40%) can be justified with the fact that the reaction time was relatively shorter and lesser temperature regarding Cellulose 1. As per these findings, acid concentration, in addition to other variables such as reaction time and temperature also influences CrI and L2 values (Table 3.8 and Table 3.9).

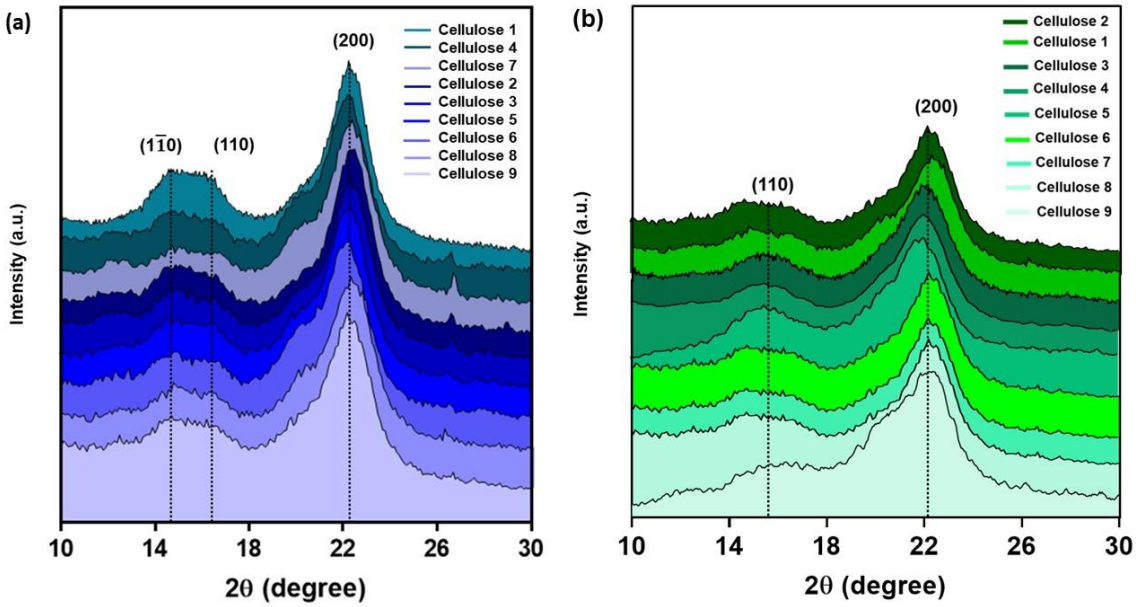

Fig. 3.8. *XRD spectra of nine cellulose samples obtained under different hydrolysis conditions from S. spontaneum (a) and banana peduncle (b).*

Herein the CrI of extracted cellulose is closely related to the lignin and hemicellulose contents. Chavez-Guerrero et al. [61] reported that removing non-cellulosic components using acid hydrolysis slackens the entangled cellulose fibers and increases the CrI. This facilitates fibrillation and promotes enzymatic digestibility and saccharification thereby increasing the potential for biofuel production. Furthermore, CrI is not a self-regulating element. An increased CrI is often accompanied by a reduction in particle size and a resultant increase in the surface area available for enzymatic digestibility [57].

Table 3.8. *Crystallinity parameters of nine cellulose samples of S. spontaneum obtained under different hydrolysis conditions.*

Sample	d-spacing(nm)			Crystallite size (nm)			CrI (%)
	d1	d2	d3	L1	L2	L3	
Cellulose 1	0.1	0.11	0.15	19.92	33.64	34.16	74.06
Cellulose 2	0.1	0.11	0.15	13.19	41.61	32.19	73.96
Cellulose 3	0.1	0.11	0.15	15.84	41.74	26.97	69.69
Cellulose 4	0.1	0.11	0.15	16.16	34.45	22.41	71.44
Cellulose 5	0.1	0.11	0.15	16.16	41.74	22.94	69.69
Cellulose 6	0.1	0.11	0.15	16.86	42.19	20.16	67.33
Cellulose 7	0.1	0.11	0.15	14.67	37.74	23.92	69.94
Cellulose 8	0.1	0.11	0.15	17.22	37.74	20.8	65.61
Cellulose 9	0.1	0.11	0.15	15.53	49.62	22.48	64.34

Table 3.9. *Crystallinity parameters of nine cellulose samples of banana peduncle obtained under different hydrolysis conditions.*

Sample	d-spacing(nm)		Crystallite size (nm)		CrI (%)
	d1	d2	L1	L2	
Cellulose 1	0.11	0.15	32.51	51.11	64.66
Cellulose 2	0.1	0.15	19.62	64.03	65.32
Cellulose 3	0.1	0.15	30.98	63.09	64.62
Cellulose 4	0.1	0.15	29.6	61.62	64
Cellulose 5	0.1	0.15	36.67	72.18	63.83
Cellulose 6	0.1	0.15	29.79	61.91	63.57
Cellulose 7	0.1	0.15	35.02	40.94	63.71
Cellulose 8	0.1	0.15	27.88	60.42	63.48
Cellulose 9	0.11	0.15	82.34	71.44	63.4

Thermogravimetric curves, derivative thermograms, and the thermal parameters of the 9 cellulose samples obtained from *S. spontaneum* and banana peduncle under different hydrolysis conditions are shown in Fig. 3.9 a, b, c, and d and presented in Table 3.9, respectively. The first degradation phase due to the evaporation of moisture content and volatile materials is shown by all the samples between 60°C to 150°C. As expected from the XRD analyses the degradation temperature decreases with an increase in the acid concentration. This was probably due to the presence of sulfate groups bound on the surface of cellulose that decreased the thermal stability of the isolated celluloses. On the other hand, the other two parameters (reaction time and temperature) were also seen to play crucial roles in the degradation temperatures of the celluloses.

From Fig. 3.9 a and c, it is seen that for *S. spontaneum* the initial decomposition temperature, as well as degradation peak temperature, decreases from Cellulose 1-3, Cellulose 4-6, and Cellulose 6-9. A similar observation has been observed for banana peduncle as can be seen in Fig. 3.9 b and d. This is related to the high reaction time and high temperature that probably degrades the crystalline cellulose and thereby decreasing the thermal stability. However, the increase in initial decomposition temperature and a degradation peak temperature of Cellulose 4 compared to Cellulose 3 and Cellulose 7 compared to Cellulose 6 in the case of *S. spontaneum* is attributed to the fact that although the acid concentrations are high in the latter two cases, the reaction temperature was considerably lower in Cellulose 4 conditions and shorter reaction time in Cellulose 7 conditions (Table 3.10). At 400°C almost all cellulose is pyrolyzed, and weight loss after that is evidence of the presence of residual non-cellulosic matter which was observed in Cellulose 3, Cellulose 6, and Cellulose 8 of banana peduncle (Fig. 3.9 d). Moreover, the char residue weight for Cellulose 1 was 7.67% for *S. spontaneum* and 3.25% for banana peduncle which was observed to be increased progressively with an increase in acid concentrations in both cases. This is possibly due to the presence of high sulfate ester groups on celluloses obtained under highly acidic conditions that act as flame retardant compounds. These findings are in full agreement with the values obtained by XRD analysis (Fig. 3.8 a and b).

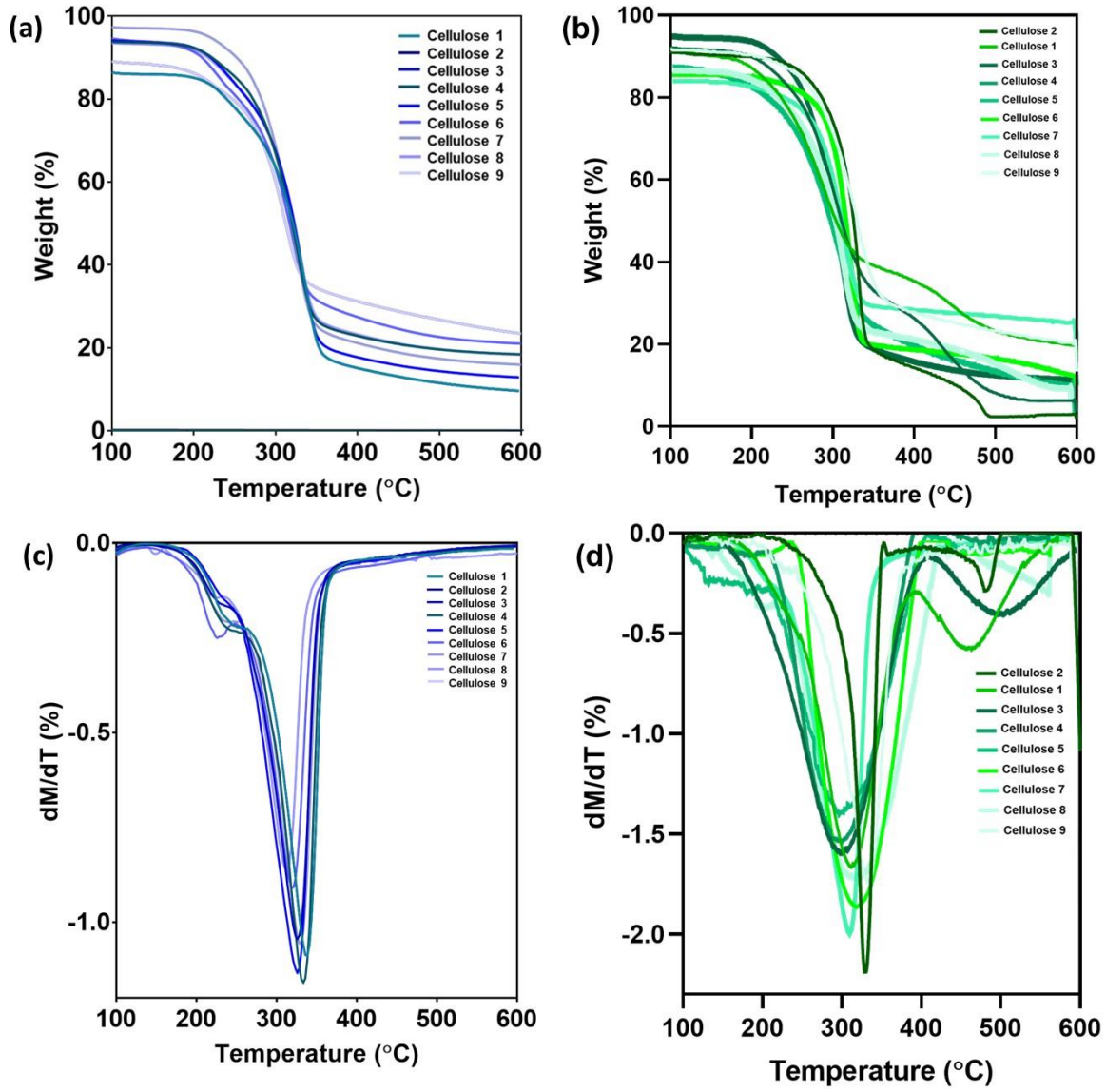

Fig. 3.9. *TGA and DTG curves of nine cellulose samples obtained from S. spontaneum (a and c) and banana peduncle (b and d) under different hydrolysis conditions.*

Table 3.10. *Weight loss and degradation temperatures of nine cellulose samples obtained from S. spontaneum and banana peduncle under different hydrolysis conditions.*

S. spontaneum				
Sample	**$T_{initial}$ (°C)**	**T_{peak} (°C)**	**W_{loss} (%)**	**$W_{residue}$(%)**
Cellulose 1	290	338	80	7.67
Cellulose 2	282	338	79	8.5
Cellulose 3	270	325	77.5	17.5
Cellulose 4	277	336	81.5	12
Cellulose 5	262	325	81.5	15.5
Cellulose 6	252	320	73.5	21
Cellulose 7	285	328	76	17.5
Cellulose 8	263	308	66	23
Cellulose 9	259	305	64.7	14.3

Banana peduncle				
Sample	**$T_{initial}$ (°C)**	**T_{peak} (°C)**	**W_{loss} (%)**	**$W_{residue}$ (%)**
Cellulose 1	293	315	60	19.1
Cellulose 2	293	325	80.33	3.25
Cellulose 3	278	305	67.5	6.3
Cellulose 4	295	300	80	12
Cellulose 5	293	298	79	10.2
Cellulose 6	290	315	72.5	12.1
Cellulose 7	274	310	76	24.1
Cellulose 8	278	312	70	9.8
Cellulose 9	287	320	68.5	20.2

3.4. Conclusion

The current chapter describes the development of an environment-friendly method for the effective extraction of cellulose from *S. spontaneum* and banana agrowastes. The extraction was carried out through the integrated treatment of alkali (NaOH), chlorine-free bleaching (H_2O_2), and acid hydrolysis (H_2SO_4). The influence of hydrolysis conditions was analyzed by applying a Taguchi orthogonal array design. Characterization results showed that re-optimizing the acid hydrolysis parameters facilitated high-yield celluloses bearing a low DP of 100-155, thus increasing the enzymatic efficiency. The extracted cellulose had an excellent cellulose content of ~83% from *S. spontaneum* and ~81% from banana peduncle, under the optimum processing conditions showing that the treatment effectively eliminated hemicellulose and lignin. FTIR results showed the cellulosic structure of cellulose and also

indicated the removal of a considerable amount of lignin and hemicellulose during the chemical treatments. Hydrolysis with a lower acid concentration in addition to the chlorine-free bleaching process made the extraction to be environmentally benign with the ensuing savings of toxic chemicals. Thus, this method can be applied to other lignocellulosic sources as well. XRD analysis confirmed the crystalline structure of the isolated cellulose, while TGA presented purity in terms of thermal stability. The morphological analysis demonstrated rod-shaped fibers of the cellulose and further uniformity in the structure of cellulose was obtained after acid hydrolysis. From the current study, it can be concluded that *S. spontaneum* and banana peduncle are promising sources for the production of cellulose with high yield and purity, using this economically viable and environmentally friendly procedure.

References

[1] Tingaut, P., Zimmermann, T., and Sèbe, G. Cellulose nanocrystals and microfibrillated cellulose as building blocks for the design of hierarchical functional materials. *Journal of Materials Chemistry*, 22(38):20105-20111, 2012.

[2] Li, R., Fei, J., Cai, Y., Li, Y., Feng, J., and Yao, J. Cellulose whiskers extracted from mulberry: A novel biomass production. *Carbohydrate polymers*, 76(1):94-99, 2009.

[3] Gholampour, A., and Ozbakkaloglu, T. A review of natural fiber composites: Properties, modification and processing techniques, characterization, applications. *Journal of Materials Science*, 55(3):829-892, 2020.

[4] Fan, G., Wang, M., Liao, C., Fang, T., Li, J., and Zhou, R. Isolation of cellulose from rice straw and its conversion into cellulose acetate catalyzed by phosphotungstic acid. *Carbohydrate Polymers*, 94(1):71-76, 2013.

[5] Shin, H. K., Jeun, J. P., Kim, H. B., and Kang, P. H. Isolation of cellulose fibers from kenaf using electron beam. *Radiation Physics and Chemistry*, 81(8):936-940, 2012.

[6] Kalita, E., Nath, B. K., Deb, P., Agan, F., Islam, M. R., and Saikia, K. High quality fluorescent cellulose nanofibers from endemic rice husk: Isolation and characterization. *Carbohydrate Polymers*, 122:308-313, 2015.

[7] Alle, M., Bandi, R., Lee, S. H., and Kim, J. C. Recent trends in isolation of cellulose nanocrystals and nanofibrils from various forest wood and nonwood products and their application. In *Nanomaterials for Agriculture and Forestry Applications*, pages 41-80. Elsevier, 2020.

[8] Mahmood, N., Yuan, Z., Schmidt, J., and Xu, C. C. Depolymerization of lignins and their applications for the preparation of polyols and rigid polyurethane foams: A review. *Renewable and Sustainable Energy Reviews*, 60:317-329, 2016.

[9] Chandel, A. K., Narasu, M. L., Chandrasekhar, G., Manikyam, A., and Rao, L. V. Use of *Saccharum spontaneum* (wild sugarcane) as biomaterial for cell immobilization and modulated ethanol production by thermotolerant *Saccharomyces cerevisiae* VS3. *Bioresource Technology*, 100(8):2404-2410, 2009.

[10] Scordia, D., Cosentino, S. L., and Jeffries, T. W. Second generation bioethanol production from *Saccharum spontaneum* L. ssp. *aegyptiacum* (Willd.) Hack. *Bioresource Technology*, 101(14):5358-5365, 2010.

[11] Chaudhary, G., Singh, L. K., and Ghosh, S. Alkaline pretreatment methods followed by acid hydrolysis of *Saccharum spontaneum* for bioethanol production. *Bioresource Technology*, 124:111-118, 2012.

[12] Singh, L. K., Majumder, C. B., and Ghosh, S. Bioconversion of hemicellulosic fraction of perennial Kans grass (*Saccharum spontaneum*) biomass to ethanol by *Pichia stipitis*: a kinetic study. *International Journal of Green Energy*, 9(5):409-420, 2012.

[13] Barman, A., Shrivastava, N. K., Khatua, B. B., and Ray, B. C. Green composites based on high-density polyethylene and *Saccharum spontaneum*: Effect of filler content on morphology, thermal, and mechanical properties. *Polymer Composites*, 36(12):2157-2166, 2015.

[14] Barman, A., Shrivastava, N. K., Khatua, B. B., and Ray, B. C. Effect of filler content on the properties of polypropylene/*Saccharum spontaneum* green composite. *Polymer-Plastics Technology and Engineering*, 54(12):1231-1240, 2015.

[15] Devnani, G. L., and Sinha, S. Extraction, characterization and thermal degradation kinetics with activation energy of untreated and alkali treated *Saccharum spontaneum* (Kans grass) fiber. *Composites Part B: Engineering*, 166:436-445, 2019.

[16] Sharma, A. K., Godiyal, R., and Thapliyal, B. P. Kans grass-a promising raw material for papermaking. *Cellulose Chemistry and Technology*, 53(7-8):747-753, 2019.

[17] Redondo-Gómez, C., Rodríguez Quesada, M., Vallejo Astúa, S., Murillo Zamora, J. P., Lopretti, M., and Vega-Baudrit, J. R. Biorefinery of biomass of agro-industrial banana waste to obtain high-value biopolymers. *Molecules*, 25(17):3829, 2020.

[18] Imteaz, M. A., Hossain, A. S., and Bayatvarkeshi, M. A mathematical modelling framework for quantifying production of biofuel from waste banana. *Environment, Development and Sustainabilty*, 61:1-12, 2021.

[19] Cutz, L., Haro, P., Santana, D., and Johnsson, F. Assessment of biomass energy sources and technologies: The case of Central America. *Renewable & Sustainable Energy Reviews*, 58:1411-1431, 2016.

[20] Sun, S. F., Yang, H. Y., Yang, J., Wang, D. W., and Shi, Z. J. Integrated treatment of perennial ryegrass: structural characterization of hemicelluloses and improvement of enzymatic hydrolysis of cellulose. *Carbohydrate Polymers*, 254:117257, 2021.

[21] Behera, S., Arora, R., Nandhagopal, N., and Kumar, S. Importance of chemical pretreatment for bioconversion of lignocellulosic biomass. *Renewable and Sustainable Energy Reviews,* 36:91–106, 2014.

[22] Boufi, S., and Chaker, A. Easy production of cellulose nanofibrils from corn stalk by a conventional high-speed blender. *Industrial Crops and Products,* 93:39–47, 2016.

[23] Haafiz, M. M., Eichhorn, S. J., Hassan, A., and Jawaid, M. Isolation and characterization of microcrystalline cellulose from oil palm biomass residue. *Carbohydrate Polymer*, 93:628–634, 2013.

[24] Maiti, S., Jayaramudu, J., Das, K., Reddy, S. M., Sadiku, R., Ray, S. S., and Liu, D. Preparation and characterization of nano-cellulose with new shape from different precursor. *Carbohydrate Polymer*, 98:562–567, 2013.

[25] Baruah, J., Chaliha, C., Kalita, E., Nath, B. K., Field, R. A., and Deb, P. Modelling and optimization of factors influencing adsorptive performance of agrowaste-derived Nanocellulose Iron Oxide Nanobiocomposites during remediation of Arsenic contaminated groundwater. *International Journal of Biological Macromolecules,* 164:53-65, 2020.

[26] Baruah, J., Deka, R. C., and Kalita, E. Greener production of microcrystalline cellulose (MCC) from *Saccharum spontaneum* (Kans grass): Statistical optimization. *International Journal of Biological Macromolecules,* 154:672-682, 2020.

[27] He, F., Chen, J., Gong, Z., Xu, Q., Yue, W., and Xie, H. Dissolution pretreatment of cellulose by using levulinic acid-based protic ionic liquids towards enhanced enzymatic hydrolysis. *Carbohydrate Polymers,* 269*:*118271, 2021.

[28] Baruah, J., Nath, B. K., Sharma, R., Kumar, S., Deka, R. C., Baruah, D. C., and Kalita, E. Recent trends in the pretreatment of lignocellulosic biomass for value-added products. *Frontiers in Energy Research*, 6:141, 2018.

[29] Zhang, M. F., Qin, Y. H., Ma, J. Y., Yang, L., Wu, Z. K., Wang, T. L., Wang, G. W., and Wang, C. W. Depolymerization of microcrystalline cellulose by the combination of ultrasound and Fenton reagent. *Ultrasonics Sonochemistry*, 31:404-408, 2016.

[30] Cherian, B. M., Leão, A. L., De Souza, S. F., Thomas, S., Pothan, L. A., and Kottaisamy, M. Isolation of nanocellulose from pineapple leaf fibres by steam explosion. *Carbohydrate Polymers*, 81(3):720-725, 2010.

[31] Adel, A. M., Abd El-Wahab, Z. H., Ibrahim, A. A., and Al-Shemy, M. T. Characterization of microcrystalline cellulose prepared from lignocellulosic materials. Part II: Physicochemical properties. *Carbohydrate Polymers,* 83(2):676-687, 2011.

[32] Ibrahim, M. M., El-Zawawy, W. K., Jüttke, Y., Koschella, A., and Heinze, T. Cellulose and microcrystalline cellulose from rice straw and banana plant waste: preparation and characterization. *Cellulose*, 20(5):2403-2416, 2013.

[33] do Nascimento, D. M., Almeida, J. S., Vale, M. D. S., Leitão, R. C., Muniz, C. R., de Figueirêdo, M. C. B., Morais, J. P. S., and Rosa, M. D. F. A comprehensive approach for obtaining cellulose nanocrystal from coconut fiber. Part I: Proposition of technological pathways. *Industrial Crops and Products,* 93:66-75, 2016.

[34] Cavali, M., Soccol, C. R., Tavares, D., Torres, L. A. Z., de Andrade Tanobe, V. O., Zandoná Filho, A., and Woiciechowski, A. L. Effect of sequential acid-alkaline treatment on physical and chemical characteristics of lignin and cellulose from pine (*Pinus* spp.) residual sawdust. *Bioresource Technology,* 316:123884, 2020.

[35] Gazliya, N., and Aparna, K. Microwave-assisted alkaline delignification of banana peduncle. *Journal of Natural Fibers*, 18:664-673, 2021.

[36] Onukwuli, O. D., Ezeh, E. M., and Odera, R. S. Effect of different chemical treatment on the properties of banana peduncle fibres. *Journal of the Chinese Advanced Materials Society*, 6:755-765, 2018.

[37] Baruah, J., Bardhan, P., Mukherjee, A. K., Deka, R. C., Mandal, M., and Kalita, E. Integrated pretreatment of banana agrowastes: Structural characterization and enhancement of enzymatic hydrolysis of cellulose obtained from banana peduncle. *International Journal of Biological Macromolecules*, 201:298-307, 2022.

[38] Abdel-Halim, E. Chemical modification of cellulose extracted from sugarcane bagasse: Preparation of hydroxyethyl cellulose. *Arabian Journal of Chemistry,* 7:362-371, 2014.

[39] Alemdar, A., and Sain, M. Isolation and characterization of nanofibers from agricultural residues–Wheat straw and soy hulls. *Bioresource Technology*, 99:1664-1671, 2008.

[40] de Carvalho Benini, KCC., Voorwald, H. J. C., Cioffi, M. O. H., Rezende, M. C., and Arantes, V. Preparation of nanocellulose from *Imperata brasiliensis* grass using Taguchi method. *Carbohydrate Polymers*, 192:337-346, 2018.

[41] Ilyas, R. A., Sapuan, S. M., and Ishak, M. R. Isolation and characterization of nanocrystalline cellulose from sugar palm fibres (*Arenga Pinnata*). *Carbohydrate Polymers*, 181:1038-1051, 2018.

[42] Abraham, E., Deepa, B., Pothan, L.A., Jacob, M., Thomas, S., Cvelbar, U., and Anandjiwala, R. Extraction of nanocellulose fibrils from lignocellulosic fibres: A novel approach. *Carbohydrate Polymers*, 86:1468-1475, 2011.

[43] Qiao, D., Liu, J., Ke, C., Sun, Y., Ye, H., and Zeng, X. Structural characterization of polysaccharides from *Hyriopsis cumingii*. *Carbohydrate Polymers*, 82:1184-1190, 2010.

[44] Kian, L. K., Jawaid, M., Ariffin, H., and Alothman, O. Y. Isolation and characterization of microcrystalline cellulose from roselle fibers. *International Journal of Biological Macromolecules*, 103:931-940, 2017.

[45] Hussin, M. H., Pohan, N. A., Garba, Z. N., Kassim, M. J., Rahim, A. A., Brosse, N., Yemloul, M., Fazita, M. N., and Haafiz, M. M. Physicochemical of microcrystalline cellulose from oil palm fronds as potential methylene blue adsorbents. *International Journal of Biological Macromolecules*, 92:11-19, 2016.

[46] Li, W., Zhang, Y., Li, J., Zhou, Y., Li, R., and Zhou, W. Characterization of cellulose from banana pseudo-stem by heterogeneous liquefaction. *Carbohydrate Polymers*, 132:513-519, 2015.

[47] Chávez-Guerrero, L., Vazquez-Rodriguez, S., Salinas-Montelongo, J. A., Roman-Quirino, L. E., and García-Gómez, N. A. Preparation of all-cellulose composites with optical transparency using the banana pseudostem as a raw material. *Cellulose*, 26:3777-3786, 2019.

[48] Flores-Jerónimo, G., Silva-Mendoza, J., Morales-San Claudio, P. C., Toxqui-Terán, A., Aguilar-Martínez, J. A., and Chávez-Guerrero, L. Chemical and Mechanical Properties of Films Made of Cellulose Nanoplatelets and Cellulose Fibers Obtained from Banana Pseudostem. *Waste and Biomass Valorization*, 12:5715-5723, 2021.

[49] Harini, K., Ramya, K., and Sukumar, M. Extraction of nano cellulose fibers from the banana peel and bract for production of acetyl and lauroyl cellulose. *Carbohydrate Polymers*, 201:329-339, 2018.

[50] Meng, F., Zhang, X., Yu, W., and Zhang, Y. Kinetic analysis of cellulose extraction from banana pseudo-stem by liquefaction in polyhydric alcohols. *Industrial Crops and Products*, 137:377-385, 2019.

[51] Shi, Y., Xia, X., Li, J., Wang, J., Zhao, T., Yang, H., Jiang, J., and Jiang, X. Solvolysis kinetics of three components of biomass using polyhydric alcohols as solvents. *Bioresource Technology*, 221:102-110, 2016.

[52] Manzato, L., Rabelo, L. C. A., de Souza, S. M., da Silva C. G., Sanches, E. A., Rabelo, D., Mariuba, L. A. M., and Simonsen, J. New approach for extraction of cellulose from tucumã's endocarp and its structural characterization. *Journal of Molecular Structure*, 1143:229-234, 2017.

[53] Nazir, M. S., Wahjoedi, B. A., Yussof, A. W., and Abdullah, M. A. Eco-friendly extraction and characterization of cellulose from oil palm empty fruit bunches. *BioResources*, 8:2161-2172, 2013.

[54] Hafid, H. S., Omar, F. N., Zhu, J., and Wakisaka, M. Enhanced crystallinity and thermal properties of cellulose from rice husk using acid hydrolysis treatment. *Carbohydrate Polymers*, 260:117789, 2021.

[55] Sun, J. X., Sun, X. F., Zhao, H., and Sun, R. C. Isolation and characterization of cellulose from sugarcane bagasse. *Polymer Degradation and Stability*, 84:331-339, 2004.

[56] Bicu, I., and Mustata, F. Cellulose extraction from orange peel using sulfite digestion reagents. *Bioresource Technology*, 102:10013-10019, 2011.

[57] Zhao, X., Zhang, L., and Liu, D. Biomass recalcitrance. Part I: the chemical compositions and physical structures affecting the enzymatic hydrolysis of lignocellulose. *Biofuels Bioproducts and Biorefining*, 6:465-482, 2012.

[58] Corrêa, A. C., de Morais Teixeira, E., Pessan, L. A., and Mattoso, L. H. C. Cellulose nanofibers from curaua fibers. *Cellulose*, 17(6):1183-1192, 2010.

[59] Habibi, Y., and Vignon, M. R. Optimization of cellouronic acid synthesis by TEMPO- mediated oxidation of cellulose III from sugar beet pulp. *Cellulose*, 15(1):177-185, 2008.

[60] Megashah, L. N., Ariffin, H., Zakaria, M. R., Hassan, M. A., Andou, Y., and Padzil, F. N. M. Modification of cellulose degree of polymerization by superheated steam treatment for versatile properties of cellulose nanofibril film. *Cellulose*, 27:7417-7429, 2020.

[61] Chávez-Guerrero, L., Silva-Mendoza, J., Toxqui-Terán, A., Vega-Becerra, O. E., Salinas-Montelongo, J. A., and Pérez-Camacho, O. Direct observation of

endoglucanase fibrillation and rapid thickness identification of cellulose nanoplatelets using constructive interference. *Carbohydrate Polymers,* 254:117463, 2021.